

Viscoelastic relaxation in oriented semicrystalline polymers

T. S. Chow and A. C. Van Laeken

Xerox Webster Research Center, 800 Phillips Road, 0114-39D, Webster, NY 14580, USA

(Received 11 August 1990; accepted 12 November 1990)

This paper presents a theoretical and experimental investigation of the basic mechanism controlling viscoelastic relaxation in oriented semicrystalline poly(ethylene terephthalate) (PET). We have analysed the anisotropic elastic moduli, creep behaviour and structural relaxation. The master creep curves and shift factors are constructed. The study helps us to separate the crystalline and amorphous contributions to the micro-deformation in oriented films. We find that (1) the crystal orientation and shape define the unrelaxed anisotropic moduli, and (2) the relaxation timescale is mainly determined by the amorphous region within PET. The calculation also reveals that the relaxation-time spectrum is very broad due to the presence of crystallites. A comparison between the theory and experiment is made.

(Keywords: orientation; semicrystalline poly(ethylene terephthalate); creep compliance; anisotropic moduli; time-temperature superposition)

INTRODUCTION

A large amount of viscoelastic data for semicrystalline poly(ethylene terephthalate) (PET) films have been reported¹⁻⁵. Time-temperature superposition has been applied to unoriented and biaxially oriented PET films. In general, orientation has a strong effect on the mechanical properties of semicrystalline polymers⁵⁻⁸. Although many useful experimental observations have been made, progress has been slow in understanding the non-equilibrium mechanism responsible for the time and temperature behaviour. This is the topic of the present paper.

We shall choose uniaxially oriented PET as a model material for our theoretical and experimental investigations into the fundamental mechanism controlling viscoelastic relaxation, by utilizing the theories developed recently⁸⁻¹⁰. The creep compliances in both directions, parallel and perpendicular to the oriented crystallites, will be measured. From the data, time-temperature superposition master curves are generated. They are then interpreted theoretically as a function of orientation, crystal shape, degree of crystallinity and the non-equilibrium glassy state, which will be determined mainly by the local motion of holes⁹ in the amorphous region of PET.

It is well known that the temperature dependence of viscoelastic relaxation data can be described by the Williams-Landel-Ferry (WLF) equation^{11,12} for $T > T_g$. In the glassy state, the departure from a WLF temperature dependence for the relaxation timescale (shift factor) will be calculated. This theoretical interpretation will then be extended to describe the relaxation in biaxially oriented PET.

MEASUREMENTS

Measurements reported here were carried out on uniaxially and biaxially oriented films. The former was

prepared by uniaxial stretching at a temperature near 146°C, and the latter was the biaxially oriented film (Melinex) manufactured by ICI. The thickness of PET films is close to 76 μm (3 mil). The morphology of non-crystalline materials depends on the temperature of crystallization and draw conditions^{13,14}.

Using a differential scanning calorimeter (DSCII), we find that there is no difference between the uniaxially and biaxially oriented PET in terms of the degree of crystallinity (ϕ), the glass transition temperature (T_g) and the melting temperature (T_m). When samples are scanned from 290 to 560 K, at the rate of 20°C min⁻¹, we obtained $T_g = 78^\circ\text{C}$, $T_m = 244^\circ\text{C}$ and $\phi = 0.33$. The degree of crystallinity is calculated as the ratio of heat of melting per gram¹⁵ of the semicrystalline PET and of 100% crystalline PET (from literature data).

Creep measurements were performed using a Dynastat Transient and Viscoelastic Analyzer. The sample's dimensions are 38.5 mm × 19 mm × 0.076 mm. Transient measurements are made by applying a 450 g tensile force, and measuring the change in sample length as a function of time (500 s) and temperature (25–150°C). Data were obtained for each sample at discrete temperatures. Prior to each measurement, the film was equilibrated for 10 min at each temperature. Figures 1 and 2 represent, respectively, the creep compliance of oriented PET film in the direction parallel and perpendicular to the direction of uniaxial stretching. In each figure, the test parameters are time and temperature and, for clear presentation, we do not show all the collected data. The master creep curves and shift factors can be generated from the data using the appropriate algorithm in the instrument's microprocessor. We shall return to this later.

ANISOTROPIC MODULI

The effect of orientation on the unrelaxed tensile moduli of semicrystalline polymers can be described by composite models^{3,7,8}. Consider a system filled with uniaxially oriented non-spherical particles; this two-

Paper presented at Speciality Polymers '90, 8-10 August 1990, The Johns Hopkins University, Baltimore, MD, USA

0032-3861/91/101798-05

© 1991 Butterworth-Heinemann Ltd.

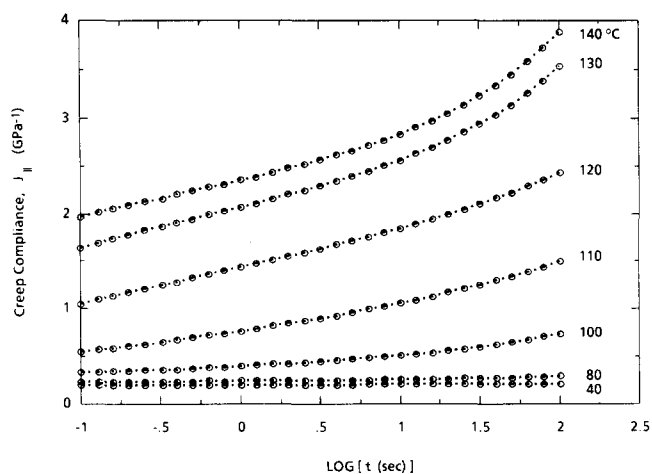


Figure 1 Measured creep compliance of the uniaxially oriented film in the direction parallel to the oriented crystallites as a function of time and temperature

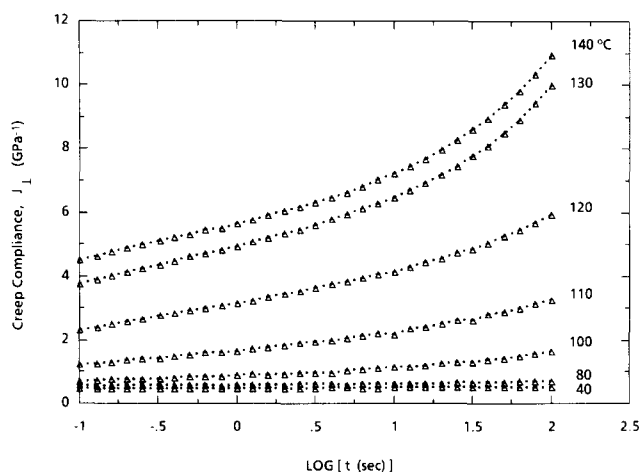


Figure 2 Measured creep compliance of the uniaxially oriented film in the direction perpendicular to the oriented crystallites as a function of time and temperature

phase heterogeneous material is anisotropic in nature. The anisotropic crystal shape effect is characterized by the ratio of major to minor axes, $\rho = c/a$, of a spheroid. The Young's modulus of a semicrystalline polymer in the direction parallel to the major c axis is given by⁸:

$$\frac{E_{||}^{(0)}}{E_2} = 1 + \frac{(k_1/k_2 - 1)G_1 + 2(\mu_1/\mu_2 - 1)K_1\phi}{2K_1G_3 + G_1K_3} \quad (1)$$

where $k = E/3(1 - 2\nu)$ is the bulk modulus, $\mu = E/2(1 + \nu)$ is the shear modulus, ν is Poisson's ratio, the subscripts 1 and 2 identify the crystalline and amorphous phases, respectively, and:

$$K_i = 1 + (k_1/k_2 - 1)(1 - \phi)\alpha_i \quad (2)$$

$$G_i = 1 + (\mu_1/\mu_2 - 1)(1 - \phi)\gamma_i \quad (3)$$

where $i = 1, 3$, and α_i and γ_i are functions of the aspect ratio ρ and Poisson's ratio ν_2 of the amorphous PET (see Appendix).

The effective Young's modulus in the perpendicular direction is⁸:

$$\frac{E_{\perp}^{(0)}}{E_2} = 1 + \frac{(k_1/k_2 - 1)G_3 + (\mu_1/\mu_2 - 1)(G_3\xi + K_3\xi)}{2K_1G_3 + G_1K_3} \phi \quad (4)$$

where

$$\xi = \frac{K_1}{1 + 2(\mu_1/\mu_2 - 1)(1 - \phi)S_{1212}} \quad (5)$$

$$\zeta = \frac{1 + (\mu_1/\mu_2 - 1)(1 - \phi)(S_{1111} - S_{3311})}{1 + 2(\mu_1/\mu_2 - 1)(1 - \phi)S_{1212}} \quad (6)$$

where S_{ijkl} is Eshelby's tensor¹⁶ and is also a function of ρ and ν_2 (see Appendix).

Equations (1) and (4) are found to be good expressions⁸ for describing the anisotropic effect on the elastic moduli of uniaxially oriented semicrystalline polymers. No adjusting parameters are needed in these equations. Consider crystalline and amorphous PET with properties: $E_1 = 69$ GPa, $\nu_1 = 0.22$ and $E_2 = 2.3$ GPa, $\nu_2 = 0.35$. The relative Young's moduli parallel and perpendicular to the orientation direction (c axis) are shown in Figure 3. The points are data measured using an Instron at the strain rate of 0.02 min^{-1} .

CREEP COMPLIANCES

Semicrystalline polymers are not in thermodynamic equilibrium. The change in the non-equilibrium glassy state (δ) and its slow relaxation define the viscoelastic response. The tensile relaxation moduli in the oriented directions can be written as:

$$E_{||}(t) = E_{||}^{(\infty)} + (E_{||}^{(0)} - E_{||}^{(\infty)}) \exp \left[- \left(\frac{t}{\tau_{||}^{(r)} a} \right)^{\beta} \right] \quad 0 < \beta \leq 1 \quad (7)$$

where t is time and $E_{||}^{(0)}$, mentioned in equation (1), is the unrelaxed modulus, which is much greater than the relaxed modulus, $E_{||}^{(\infty)}$, for $T < 146^\circ\text{C}$, the temperature under which the uniaxially oriented PET film was formed. The macroscopic relaxation is $\tau_{||}^{(r)} a$, β is the fractal exponent, and $\tau_{||}^{(r)}$ refers to the relaxation time at $T = T_r$. The reference temperature is a fixed quantity near T_g and

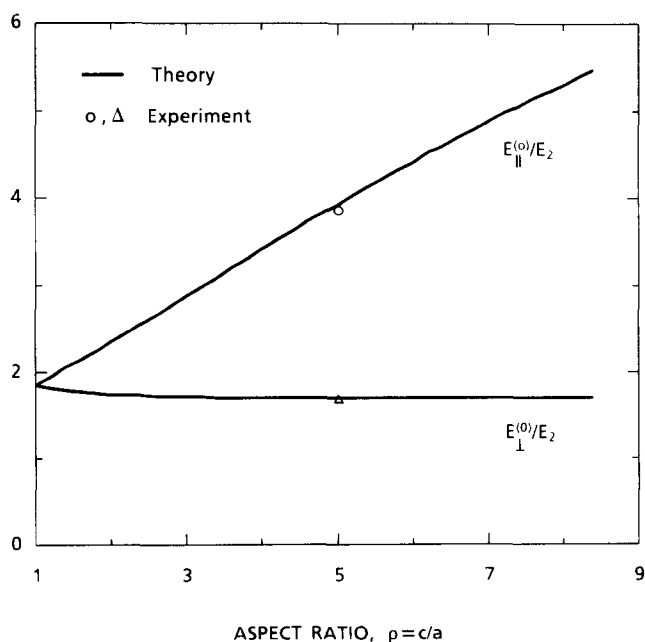


Figure 3 Relative unrelaxed tensile moduli in the parallel and perpendicular directions of the uniaxially oriented PET. The degree of crystallinity (ϕ) is 33%

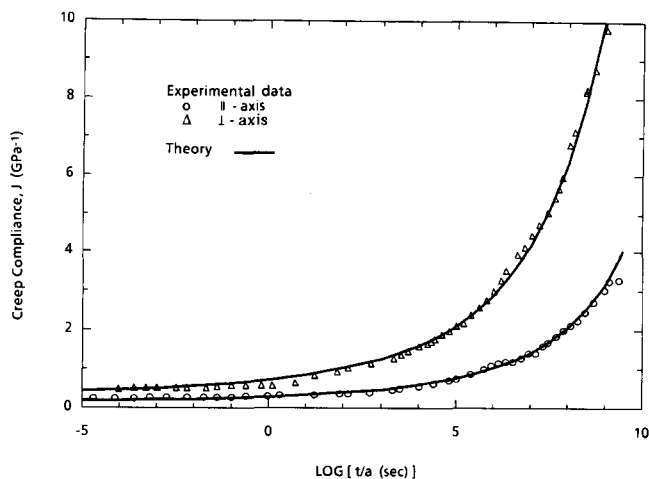


Figure 4 Comparison of the calculated (equations (7) and (8)) and the measured master creep curves in both directions for the uniaxially oriented films

$\delta=0$. The shift factor a is a function of temperature and the non-equilibrium glassy state. The relaxation modulus in the perpendicular direction can also be written in the same form as equation (7) with the subscript \parallel being replaced by the subscript \perp :

$$E_{\perp}(t) = E_{\perp}^{(\infty)} + (E_{\perp}^{(0)} - E_{\perp}^{(\infty)}) \exp \left[- \left(\frac{t}{\tau_{\perp}^{(r)} a} \right)^{\beta} \right] \quad 0 < \beta \leq 1 \quad (8)$$

where the unrelaxed modulus $E_{\perp}^{(0)}$ is now given by equation (4).

On the basis of the quasielastic method⁸, the creep compliance is the reciprocal of the relaxation modulus ($J=1/E$). A comparison between the theory and experiment for uniaxially oriented PET is carried out in *Figure 4*. The experimental points in *Figure 4* have been shifted horizontally to form the master creep compliance. The shift factor a will be discussed in the next section. The reference temperature for the master curves is 80°C. The full curves represent the theoretical calculation. Using equations (7) and (8), we have determined $\beta=0.06$, $\tau_{\parallel}^{(r)}=1.8$ s and $\tau_{\perp}^{(r)}=0.36$ s. The value of β is independent of the orientation. *Figure 4* also reveals that the timescale (t/a) for oriented PET is very broad, spanning 15 orders of magnitude.

SHIFT FACTOR

The time-temperature superposition has been extensively studied in the literature to understand the kinetics of polymer relaxation. It is well established that the linear viscoelastic response obeys the WLF¹¹ (or Doolittle¹⁷) shift function at temperatures above the glass transition temperature. For $T < T_g$, the non-equilibrium changes of the glassy state in the amorphous region of PET have to be included in the analysis.

According to our kinetic theory of glasses⁹, the temperature dependence of the equilibrium free volume (hole) fraction at temperatures both above and below T_g is given by:

$$\bar{f}(T) = f_r \exp \left[- \frac{\varepsilon}{R} \left(\frac{1}{T} - \frac{1}{T_r} \right) \right] \quad (9)$$

where ε is the mean energy of hole formation, R is the

gas constant and f_r is the reference free volume fraction at $T=T_r$. The non-equilibrium glassy state, $\delta=f-\bar{f}$, is determined by solving the kinetic equations that describe the local motion of holes in the metastable state. The solution is:

$$\delta(T, q) = - \frac{\varepsilon}{R T_0} \int_{T_0}^T \frac{\bar{f}}{T'^2} \exp \left[- \left(\frac{T-T'}{q \tau_r a(T, \delta)} \right)^{\beta} \right] dT' \quad 0 < \beta \leq 1 \quad (10)$$

where q is the cooling (<0) rate, τ_r is the reference volume relaxation time and β defines the shape of the hole energy spectrum. The numerical solution of the above equation is not affected by the initial temperature of $T_0 > T_g + 10^\circ\text{C}$. The exponent β also links the macroscopic shift factor (a) to that of the local state (λ) by^{9,10}:

$$\ln a(T, \delta) = \frac{\ln \lambda(T, \delta)}{\beta} = \frac{1}{\beta} \left(\frac{1}{\bar{f} + \delta} - \frac{1}{f_r} \right) \quad (11)$$

The presence of δ in the above equation is due to change of configurational hole entropy in the non-equilibrium glasses. For temperatures above the glass transition, we have $\delta=0$, and equation (11) becomes the Doolittle equation, which can also be written in the form of the WLF equation as:

$$\log a = - \frac{C_1(T-T_r)}{C_2 + (T-T_r)} \quad \text{for } T > T_r \quad (12)$$

where

$$C_1 = \frac{1}{2.303 \beta f_r} \quad \text{and} \quad C_2 = \frac{R T_r^2}{\varepsilon} \quad (13)$$

When the experimental a vs. T data on uniaxially oriented PET above $T_r=80^\circ\text{C}$ are analysed, equations (12) and (13) give $\varepsilon=1.34$ kcal mol⁻¹ and $\beta f_r=0.0132$. In addition to these values, we use $\beta=0.06$, which was determined in the last section, and choose $|q| \tau_r=0.1^\circ\text{C}$ in equation (10). We have shown¹⁰ that the cooling rate has little effect on the calculated slope of $\log a$ versus T in the glassy state. Equations (9)–(11) extend the prediction of the temperature dependence of the shift factor into the transition region and glassy state. The theory and experiment are compared in *Figure 5*. The experimental points, in both the parallel and perpendicular directions,

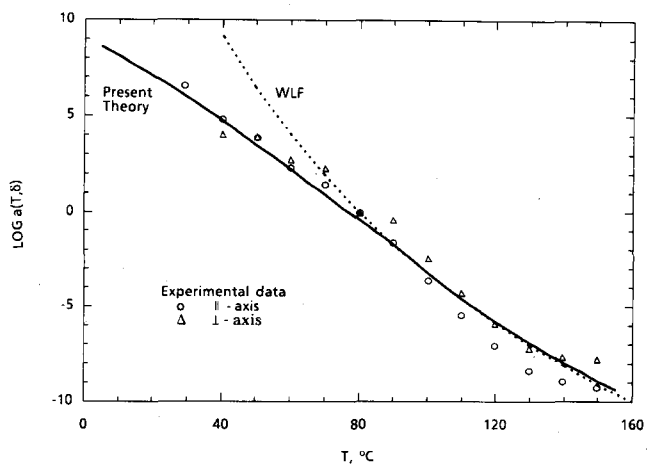


Figure 5 Comparison of the shift factors calculated from the present theory (equations (9)–(11)) and from the WLF equation (equation (12)) with experimental data for the uniaxially oriented film

correspond to those in Figure 4. The full and dotted curves represent the theoretical calculations in accordance with equations (11) and (12), respectively. Figures 4 and 5 reveal that the relaxation timescale is mainly determined by the amorphous region of PET. The mean energy of hole formation (ε) and the hole energy spectrum (β) are not affected by the anisotropic deformation. However, the hole energy spectrum, which is directly related to the distribution of the relaxation times, is very broad. The presence of the crystalline phase may have caused the slow-down of hole motions, which results in small β . The departure from a WLF temperature dependence of the shift factor starts to appear in the vicinity of the glass transition. The temperature dependence of the activation energy (ΔH) in the transition region¹⁰ can also be described by the same hole parameters:

$$\Delta H \approx (1 - \eta) \varepsilon / \beta f_r \quad (14)$$

where $\varepsilon / \beta f_r = 102.1 \text{ kcal mol}^{-1}$, and

$$\eta = -\frac{1}{\theta_r} \frac{d\delta}{dT} \quad \text{and} \quad \theta_r = \frac{\varepsilon f_r}{RT_r^2} \quad (15)$$

The physical ageing rate η , known as Struik's exponent¹⁸, increases at a slower rate in oriented PET than in most glassy polymers as the temperature decreases. It reaches 0.51 at $T = 30^\circ\text{C}$.

COMPARISON WITH BIAXIALLY ORIENTED PET

Creep compliances in two perpendicular directions of the biaxially oriented ICI Melinex were measured in exactly the same way as that for the uniaxially oriented PET. The measurement covers the same time and temperature ranges. In Figure 6, the effects of orientation and temperature on the creep behaviour of semicrystalline PET are illustrated. Since the uniaxially oriented sample was stretched at 146°C , its effect on the creep compliances is shown in Figure 6. This explains that the creep data for $t/a > 10^9 \text{ s}$ are lower than the calculated curve, which we have observed earlier in Figure 4, and suggests that the relaxed moduli ($E_{\parallel}^{(\infty)}$ and $E_{\perp}^{(\infty)}$) may no longer be negligible in the theoretical calculation of this time domain.

By the shifting of creep data of the biaxially oriented

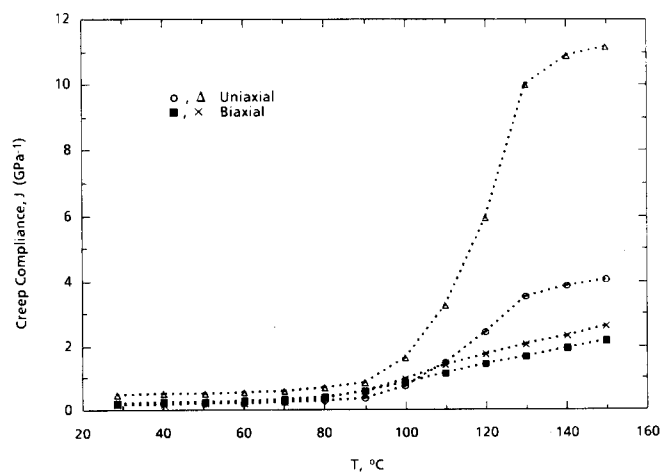


Figure 6 Creep compliance of the uniaxially and biaxially (ICI Melinex) oriented films as a function of temperature at $t = 100 \text{ s}$

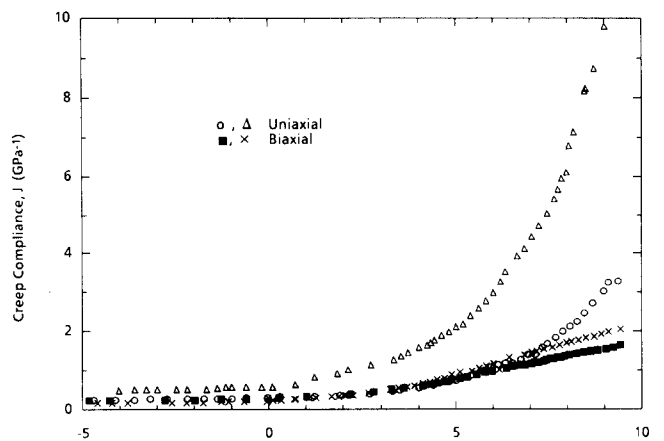


Figure 7 Master creep curves of the uniaxially and biaxially oriented PET films

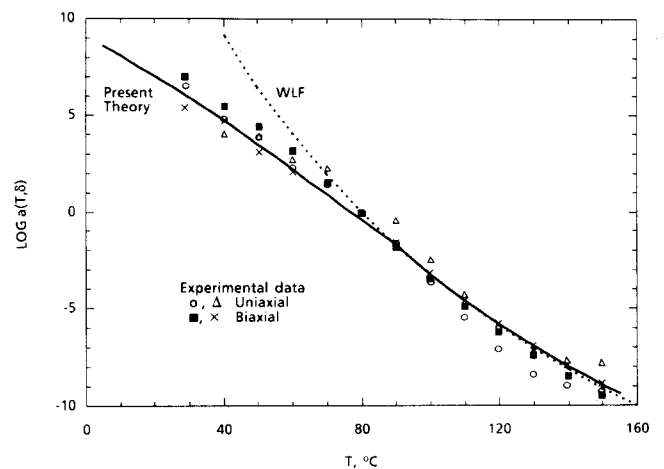


Figure 8 Shift factors of the uniaxially and biaxially oriented PET films

film, two master curves were generated, in Figure 7, where the earlier data of the uniaxially oriented film are also presented. The biaxially oriented samples show higher creep resistance over a broad temperature range. This may be related to the larger temperature-independent reference relaxation times ($\tau_{\parallel}^{(r)}$, $\tau_{\perp}^{(r)}$) in equations (7) and (8). Shift factors for biaxially oriented ICI Melinex with $T_r = 80^\circ\text{C}$ are plotted in Figure 8. Our results are in reasonable agreement with other studies of biaxially oriented films^{4,5}. The biaxial data are compared with the theoretical and experimental results for the uniaxially oriented PET already mentioned in Figure 5. Again, Figure 8 reveals that orientation has a very small effect on the shift factor (relaxation timescale) of semicrystalline PET.

CONCLUSIONS

The anisotropic master creep curves and their shift factors for uniaxially oriented semicrystalline PET are theoretically calculated and experimentally measured. Crystal orientation and shape have a strong effect on the unrelaxed tensile moduli in the parallel and perpendicular directions. However, they have a very small effect on the shift factor. The mean energy of hole formation and the hole energy spectrum are not affected by the anisotropic deformation. This suggests that the relaxation timescale is mainly determined by the amorphous region of PET.

The calculation also reveals that the hole energy spectrum, which is directly related to the distribution of the relaxation times, is very broad. The presence of the crystalline phases may have caused the slow-down of hole motions, which results in small β .

A comparison with the corresponding properties of biaxially oriented PET is also made. Measurements indicate that there is no difference in the degree of crystallinity and the glass transition temperature between the uniaxially and biaxially oriented PET samples. We have clearly shown that orientation has very little effect on the shift factor (relaxation timescale) for both uniaxially and biaxially oriented PET. Similar to amorphous and crosslinked polymers¹⁰, the departure from a WLF temperature dependence of the shift factor starts to appear in the vicinity of the glass transition. This is related to the onset of physical ageing in the amorphous region of PET.

ACKNOWLEDGEMENTS

We thank J. Mammino for providing us with the uniaxially oriented PET samples, and R. A. Mosher for d.s.c. measurements.

REFERENCES

- 1 Ward, I. M. *Polymer* 1964, **5**, 59
- 2 Hawthorne, J. M. *J. Appl. Polym. Sci.* 1981, **26**, 3317
- 3 Takayanagi, M. *Mem. Fac. Eng.* 1963, **23**, 41
- 4 Murayama, T., Dumbleton, J. H. and Williams, M. L. *J. Polym. Sci. (A-2)* 1968, **6**, 787
- 5 Vallat, M. F. and Plazek, D. J. *J. Polym. Sci. (B)* 1988, **26**, 555
- 6 Ward, I. M. 'Mechanical Properties of Solid Polymers', 2nd Edn., Wiley, New York, 1983
- 7 Mead, W. T. and Porter, R. S. *J. Appl. Phys.* 1976, **47**, 4278
- 8 Chow, T. S. *J. Mater. Sci.* 1980, **15**, 1873; *J. Polym. Sci., Polym. Phys. Edn.* 1978, **16**, 959
- 9 Chow, T. S. *Macromolecules* 1989, **22**, 701
- 10 Chow, T. S. *J. Polym. Sci. (B)* 1987, **25**, 137; *Polymer* 1988, **29**, 1447; *J. Mater. Sci.* 1990, **25**, 957
- 11 Williams, M. L., Landel, R. F. and Ferry, J. D. *J. Am. Chem. Soc.* 1955, **77**, 3701
- 12 Ferry, J. D. 'Viscoelastic Properties of Polymers', 3rd Edn., Wiley, New York, 1980
- 13 Groeninckx, G., Reynaers, H., Berghmans, H. and Smets, G. *J. Polym. Sci., Polym. Phys. Edn.* 1980, **18**, 1311

- 14 Gupta, V. B., Ramesh, C. and Gupta, A. K. *J. Appl. Polym. Sci.* 1984, **29**, 3115
- 15 Mandelkern, L. 'Crystallization of Polymers', McGraw-Hill, New York, 1964
- 16 Eshelby, J. D. *Proc. R. Soc. Lond. (A)* 1957, **241**, 376
- 17 Doolittle, A. K. *J. Appl. Phys.* 1951, **22**, 1471
- 18 Struik, L. C. E. 'Physical Aging in Amorphous Polymers and Other Materials', Elsevier, Amsterdam, 1978

APPENDIX

The pertinent parameters for equations (2), (3), (5) and (6) are listed in the following⁸:

$$\alpha_1 = 4\pi Q/3 - 2(2\pi - I)R$$

$$\alpha_3 = 4\pi Q/3 - 4(I - \pi)R$$

$$\gamma_1 = \left(\frac{4\pi}{3} - \frac{4\pi - 3I}{1 - \rho^2} \right) Q - 4(I - 2\pi)R$$

$$\gamma_3 = \left(\frac{4\pi}{3} - \frac{(4\pi - 3I)\rho^2}{1 - \rho^2} \right) Q - (4\pi - I)R$$

$$2S_{1212} = \frac{2}{3} \left(\pi - \frac{1}{4} \frac{4\pi - 3I}{1 - \rho^2} \right) Q + 2IR$$

$$S_{1111} - S_{3311} = \left(\pi - \frac{7}{12} \frac{4\pi - 3I}{1 - \rho^2} \right) Q + (4\pi - I)R$$

where

$$Q = \frac{3}{8\pi} \frac{1}{1 - \nu_2} \quad R = \frac{1}{8\pi} \frac{1 - 2\nu_2}{1 - \nu_2}$$

and

$$I = \frac{2\pi\rho}{(\rho^2 - 1)^{3/2}} [\rho(\rho^2 - 1)^{1/2} - \cosh^{-1}\rho] \quad \text{for } \rho > 1$$

When $\rho \rightarrow 1$,

$$\alpha_1 = \alpha_3 = \frac{1}{3} \frac{1 + \nu_2}{1 - \nu_2}$$

$$\gamma_1 = \gamma_3 = 2S_{1212} = S_{1111} - S_{3311} = \frac{2}{15} \frac{4 - 5\nu_2}{1 - \nu_2}$$